Published in final edited form as:
J Mol Cell Cardiol. 2011 November ; 51(5): 730–739. doi:10.1016/j.yjmcc.2011.07.028.

A full range of mouse sinoatrial node AP firing rates requires protein kinase A-dependent calcium signaling

Jie Liu[1,2], **Syevda Sirenko**[1], **Magdalena Juhaszova**[1], **Bruce Ziman**[1], **Veena Shetty**[3], **Silvia Rain**[1], **Shweta Shukla**[1], **Harold A. Spurgeon**[1], **Tatiana M. Vinogradova**[1], **Victor A. Maltsev**[1], and **Edward G. Lakatta**[1,*]

[1]Laboratory of Cardiovascular Science, Intramural Research Program, Gerontology Research Center, National Institute on Aging, National Institutes of Health, 5600 Nathan Shock Drive, Baltimore MD 21224

[3]MedStar Research Institute

Abstract

Recent perspectives on sinoatrial nodal cell (SANC)* function indicate that spontaneous sarcoplasmic reticulum (SR) Ca^{2+} cycling, i.e. an intracellular "Ca^{2+} clock," driven by cAMP-mediated, PKA-dependent phosphorylation, interacts with an ensemble of surface membrane electrogenic molecules ("surface membrane clock") to drive SANC normal automaticity. The role of AC-cAMP-PKA-Ca^{2+} signaling cascade in mouse, the species most often utilized for genetic manipulations, however, has not been systematically tested. Here we show that Ca^{2+} cycling proteins (e.g. RyR2, NCX1, and SERCA2) are abundantly expressed in mouse SAN and that spontaneous, rhythmic SR generated Local Ca^{2+} Releases (LCRs) occur in skinned mouse SANC, clamped at constant physiologic [Ca^{2+}]. Mouse SANC also exhibits a high basal level of phospholamban (PLB) phosphorylation at the PKA-dependent site, Serine16. Inhibition of intrinsic PKA activity or inhibition of PDE in SANC, respectively: reduces or increases PLB phosphorylation, and markedly prolongs or reduces the LCR period; and markedly reduces or accelerates SAN spontaneous firing rate. Additionally, the increase in AP firing rate by PKA-dependent phosphorylation by β-adrenergic receptor (β-AR) stimulation requires normal intracellular Ca^{2+} cycling, because the β-AR chronotropic effect is markedly blunted when SR Ca^{2+} cycling is disrupted. Thus, AC-cAMP-PKA-Ca^{2+} signaling cascade is a major mechanism of normal automaticity in mouse SANC.

Keywords

Sinoatrial node; Automaticity; Adenylyl cyclase-cyclic AMP-protein kinase A- Ca^{2+} signaling cascade; Ca^{2+} cycling proteins; Phospholamban phosphorylation; Local Ca^{2+} releases

*Abbreviations: AP, action potential; β-AR, β-adrenergic receptor; CSQ, calsequestrin; CT, Crista Terminalis; LCRs, Local Ca^{2+} Releases; PLB, phospholamban; RyR, ryanodine receptors; SR, sarcoplasmic reticulum; SANC, sinoatrial nodal cell; NCX, Sodium-Calcium-Exchanger

*Address correspondence to: Edward G. Lakatta, M.D., Laboratory of Cardiovascular Science, Gerontology Research Center, NIA, NIH, 5600 Nathan Shock Drive, Baltimore, Maryland 21224-6825, USA, Telephone: 410-558-8202, Fax: 410-558-8150, LakattaE@grc.nia.nih.gov.
[2]Present address: Muscle Cell Function Laboratory, School of Medical Sciences, Anderson Stuart Building (F13), University of Sydney, Sydney NSW 2006 Australia

INTRODUCTION

Recent evidence supports the hypothesis that spontaneous, rhythmic intracellular Ca^{2+} cycling acts as a partner with surface membrane ion channels to regulate automaticity of SAN pacemaker cells (SANC). Local subsarcolemmal Ca^{2+} Releases (LCRs) generated by sarcoplasmic reticulum (SR) ryanodine receptors (RyR) result in an increase in Na-Ca^{2+} exchanger current (NCX), which accelerates the diastolic depolarization. The timing of this LCR prompt of NCX inward current is a determinant of the time at which the generation of the next action potential (AP) will begin [1]. Basal SR Ca^{2+} cycling within SANC is driven by a constitutively active adenylyl cyclase-cyclic AMP-protein kinase A-Ca^{2+} (AC-cAMP-PKA-Ca^{2+}) signaling cascade, kept in check by high constitutive phosphodiesterase (PDE) activity [2, 3]. This cAMP-PKA-Ca signaling cascade targets both SR Ca^{2+} cycling molecules and surface membrane electrogenic molecules (6), thus coupling the functions of these molecules to form a robust coupled-clock system that controls normal cardiac pacemaker function.

In mouse SANC, numerous studies have demonstrated the characteristics and functional role of sarcolemmal ion channels, and have documented the effects of targeted gene modification of ion channels on automaticity in mouse SAN [4, 5]. Steady levels of mRNA for Ca^{2+} cycling protein genes in mouse SAN have been reported [6], and reports of Ca^{2+} regulation involving Ca^{2+}/calmodulin-dependent protein kinase II signaling in mouse SAN/SANC have recently appeared [7–9]. However, neither Ca^{2+} cycling protein levels, nor effects of their post-translational modification, e.g. basal state phosphorylation, are known in mouse SANC. Additionally, unlike rabbit or guinea pig SANC, in which there is strong evidence for the crucial importance of AC-cAMP-PKA signaling axis in basal normal automaticity, i.e. in the absence of autonomic receptor stimulation[10, 11], little is known about basal AC-cAMP-PKA signaling in mouse SAN, its impact on Ca^{2+} cycling, or how this might relate to normal automaticity in the mouse SAN, which exhibits a more rapid basal AP firing rate than larger mammals.

The purpose of our study is to determine: 1) the presence and location of Ca^{2+} cycling proteins in the mouse SAN tissue/cells and to quantify the levels of selected proteins, using western blots; 2) the extent of basal PKA-dependent phosphorylation in individual SANC isolated from SAN, using immuno-labeling techniques and phospholamban (PLB) phosphorylation at Serine16 as an index of PKA-dependent phosphorylation; and 3) to characterize PKA-dependent spontaneous LCRs and their dependence on PKA signaling in permeabilized SANC in which membrane clock is disabled and uncoupled from the Ca^{2+} clock; 4) the impact of modulation of SR Ca^{2+} cycling by direct inhibition of SR Ca^{2+} pumping, by disabling RyR function, or by PKA or PDE inhibition, on basal mouse SAN firing rate, or that in response to β-adrenergic receptor (β-AR) stimulation.

MATERIALS AND METHODS

Isolation of the mouse SAN

All experiments are performed on 2–4 month old male C57BL/6J mice, and all animal procedures are carried out under the guidance of the NIH animal care and animal study ethics Committee approved protocol (#409 LCS2011). For detailed methods of isolation of the mouse SAN, see online supplement.

Electrophysiological recording of SAN spontaneous pacemaking activity

The SAN preparation is fixed in a heated tissue bath and superfused with preheated Tyrode solution with or without drugs at 36 ± 0.5 °C at a rate of ~4 ml/min. To record the extracellular signals, an insulated/Teflon-coated platinum electrode with a tip of 0.25 mm

diameter is placed in the center SAN region. Real-time extracellular potentials and the firing rate of the SAN are recorded by a Neurolog system NL900D (Digitimer, Hertfordshire, UK) and stored in a PC for offline analysis.

Western blotting

SAN strips are snap-frozen in liquid nitrogen, together with an equal amount of atrial and ventricular tissue from the same heart. For western blotting experiments, SAN strips from 20 mice are pooled together for western blotting using protocol previously established [12]. In order to compare relative protein expression levels in SAN, atrial and ventricular tissue, samples of all three tissue types are included in each blot, and the same amount of total protein is loaded in each lane.

Immunohistochemistry and confocal microscopy

8 μm thick tissue sections containing the SAN region are cut perpendicularly to Crista Terminalis (CT) as described previously [13]. Tissue sections and isolated SANC are processed for immuno-staining and confocal microscopy as previously described [13]. Antibodies used in this study are listed in online supplementary data. After immunohistochemistry, cells or tissue sections are visualized with a Zeiss Laser Scanning Microscope (LSM510). Average fluorescence intensity of each SANC (excluding nuclei) is quantified and measured as an index of relative immuno-reactivity to specific antibody with ImageJ software (http://rsb.info.nih.gov/ij/) as described previously [13]. Detailed methods for immuno-labeling are provided in the online supplement.

Isolation of single SANC

Detailed methods for isolation of single SANC are provided in the online supplement. Intact mouse SANC are plated on laminin-coated (20 μg/ml) in 35 mm #zero glass bottom petri dishes (MatTek Cultureware) for 20 min to attach. After superfusion with normal Tyrode solution (with 1.8 mM Ca^{2+}), only spontaneously beating SANC are selected and then permeabilized with saponin (0.01 % for 2 min) to record Spontaneous LCRs in the line scan mode, with the scan line oriented along cell membrane as described previously[14]. See online supplementary data for details of the characterization of LCRs.

Drugs

See online supplementary data for details about drugs used in this study.

Statistics

Data are presented as mean ± S.E.M. (n = number of preparations or cells). Where applicable, a single factor ANOVA test is applied. $P<0.05$ is considered as statistically significant.

RESULTS

Molecular phenotype of Ca^{2+} cycling proteins in mouse SAN/SANC

Immuno-labeling of thin SAN tissue sections containing the SAN region (defined as HCN4-positive region [13] and neighboring atrial myocytes (at the CT) shows abundant expression of RyR2, SERCA2 and NCX1 proteins (Fig. 1A). The immuno-labeling intensity of HCN4 is highest in the central SAN region, becomes less in the peripheral SAN region, and is absent in the neighboring atrial myocardium at the CT (Fig. S2). RyR2, SERCA2 and NCX1 show similar immuno-labeling intensity in each of the three regions (Fig. S2). Figure 1B shows western blots of mouse SAN, atrial and ventricular tissue for RyR2, NCX1 and

SERCA2a. A microfilament protein, α-actinin, is used as loading control protein. Note that NCX1, SERCA2a and RyR2 are as abundant in SAN as in ventricular or atrial tissue.

Isolated, spindle shaped SANC characterized by the absence of Connexin 43 (Cx 43) immune-labeling (Fig. 2A) and exhibiting positive immuno-labeling of HCN4 (Fig. 2C) also have abundant expression of SERCA2, NCX1, and RyR2 (Fig. 2A, B, C). NCX, HCN4, RyR2 and SERCA2 immuolabeling is intense on or near the surface membrane. A similar staining pattern is found in SANC labeled with Caveolin 3 (Fig. 2D), a major type of caveolin implicated in β-AR signal transduction in rabbit SANC [15–17]. Within the sub-sarcolemmal area intense RyR immuno-labeling overlaps with that of HCN4, as indicated by yellow color in the merged image (Fig. 2C). SR calcium buffering and binding protein, calsequestrin (CSQ) also exhibits a sub-sarcolemmal distribution pattern in SANC (Fig. S3). In contrast to the sub-sarcolemmal pattern of CSQ in SANC, ventricular myocyte CSQ immuno-labeling exhibits a uniformly striated pattern (presumably due to its distribution in junctional SR) (Fig. S3). The immuno-labeling of SR proteins SERCA2 and RyR2 occurs throughout SANC body (Fig. 2A, C). Thus, the densities of surface membrane proteins (HCN4, NCX1 and Caveolin-3) and sub-sarcolemma SR calcium cycling proteins (RyR2, SERCA2 and CSQ) are highest in the sub membrane area of mouse SANC, where most calcium cycling events related to automaticity in other species occur [12, 16].

SAN pacemaking function depends on Ca^{2+} and intact SR function

The requirement for extracellular Ca^{2+} and SR Ca^{2+} cycling protein function in SAN automaticity is demonstrated in Figure 3. When the extracellular perfusion Tyrode solution (1.8 mM Ca^{2+}) is replaced by a Ca^{2+}-free solution containing the Ca^{2+} chelator, EGTA, the SAN spontaneous beating rate is dramatically reduced to a few random beats (~10 bpm) in 15–20 min (n=3) (Fig. 3A). The mouse SAN's response to caffeine, which activates RYRs and ultimately depletes SR Ca^{2+} content, is an initial increase in the average beating rate followed by a marked reduction (Fig. 3B). On average, when SR calcium content is lowered by 20 mM caffeine, the average spontaneous beating of SAN decreases by ~73%, from 404.19 ± 24.65 bpm at basal level to 108.93 ± 11.37 bpm (n=6); and in one out of seven preparations, spontaneous beating stops within 10 min (Fig. 3B). The caffeine effect is reversible when caffeine is washed (not shown).

Ryanodine, which keeps RyRs in an open state, has similar effects to those of caffeine on the spontaneous SAN beating rate (Fig. 3C). Note the instability of the beating rate early after ryanodine application. The average concentration-response of beating rate to continuous perfusion with varying ryanodine concentrations is illustrated in online supplement Figure S4A. In response to 10 μM ryanodine mouse SAN beating rate becomes reduced, from 333 ± 16 bpm to 143 ± 14 bpm (n=6, $P < 0.05$), i.e., 57 ± 4 % reduction (Figure 3C).

Specific inhibition of Ca^{2+} pumping into SR by 5 μM CPA also results in substantial decrease in the beating rate (Fig. 3D). On average, the extent of the reduction is 54.36 ± 6.54% (from 393.93 ± 15.61 bpm to 180.34 ± 15.51 bpm, n=6, $P < 0.05$; Fig. 8D). Results in Figure 3A and B indicate crucial roles of both extracellular Ca^{2+}, which is required for normal L-type Ca^{2+} channel function, and maintenance of the SR Ca^{2+}content in SAN pacemaking function. The results in Figure 3C and D indicate a crucial dependence of normal basal mouse SAN pacemaker function on normal SR Ca^{2+} cycling, including Ca^{2+} pumping into SR via SERCA and Ca^{2+} release from SR via RyRs.

Sustained basal activation of PKA-dependent signaling is linked to spontaneous basal SR Ca^{2+} cycling and to the basal SAN firing rate

To index PKA-dependent phosphorylation, we immuno-labeled isolated, single mouse SANC with antibodies against total PLB (red) and P-PLB at Ser16 site (PLB-PS16, green). Figure 4 shows examples of mouse SANC labeled with PLB antibodies in the basal state (panel A), prior to and following PKA inhibition (with either a specific PKA inhibitor peptide, PKI, or H89, panels B and C) following AC or PDE inhibition (panels D and E) and in response to β-AR stimulation by isoproterenol (panel F). Note that SANC (Fig. 4A) exhibit substantial basal PLB-P16 phosphorylation at PKA-dependent Ser16 site as indicated by strong PLB-PS16 immuno-reactivity (green). At higher magnification (Fig. S5), immunolabeling of PLB-PS16 appears highly punctuated, and differs from the (less-interrupted pattern of) immunolabeling of total PLB. Inhibition of PKA signaling by PKI or H89 suppresses basal PLB phosphorylation (Figs. 4B, C) and on average the magnitude of the reduction was about 60% (Fig. 5A). The high basal level of PLB phosphorylation in SANC (Fig. 4A) is not present in ventricular myocytes (Fig. S6). Furthermore, perturbations that have marked effects on basal PLB phosphorylation in SANC have little or no effect in ventricular myocytes (Fig. S6).

The functional importance of basal PKA-dependent phosphorylation is demonstrated by the effect of its inhibition on SAN spontaneous beating rate. When applied to freshly isolated beating SAN preparation, the PKA inhibitor H89 markedly decreases spontaneous beating rate in a concentration-dependent manner (Figs. S4A, S4B). The average reduction in beating rate was 59.18 ± 8.33% after 10 μM H89 (n=5, $P < 0.05$) (Fig. 5B). This response to H89 was not significantly changed when possible actions of acetylcholine or noradrenaline release from autonomic nerve terminals were suppressed by 10 μM atropine and 2 μM propranolol respectively. (n = 3, data not shown).

Constitutive adenylyl cyclase activity drives basal PKA-dependent phosphorylation and spontaneous beating

Following treatment of a single isolated mouse SANC with 100 μM MDL-12330 A (MDL), an AC inhibitor that reduces cAMP production [3] and cAMP-mediated PKA-dependent PLB phosphorylation at Ser16 site, the immuno-labeling of PLB PS-16 is reduced, as shown by decreased green fluorescent intensity (Fig. 4D). On average, while the total PLB, indicated by the red fluorescent signal, is unchanged, the ratio of PLB-PS16/PLB-total in SANC decreased by 38.51 ± 3.2 % from its basal level (Fig. 5A). The effect of MDL to decrease PLB PS16 phosphorylation in SANC is comparable to the inhibitory effect of PKI and H89 (Fig. 5A). This strong inhibitory effect of MDL on basal cAMP-mediated PKA-dependent phosphorylation demonstrates a critical role of basal AC activity on PKA-dependent phosphorylation. Moreover, the spontaneous beating of SAN preparation ceases (beating rate = 0 bpm) when the same amount of MDL is applied in the superfusion solution (n=3, Fig. S4B). That both MDL and PKI reduce both basal cAMP-mediated PKA-dependent phosphorylation and spontaneous beating indicates that both basal AC and PKA activity are linked to normal SAN spontaneous basal beating.

Basal PKA-dependent phosphorylation and beating rate are controlled by basal phosphodiesterase activity

A high level of PDE activity is one control mechanism of the basal AC-cAMP-PKA-Ca^{2+} signaling and beating rate of rabbit SANC [3]. A similar picture emerges in mouse SAN. Figure 4E illustrates a SANC in which PDE was inhibited by 100 μM IBMX, probed with anti-PS16 PLB antibody and PLB total antibody. On average, the broad spectrum cyclic nucleotide PDE inhibition, IBMX, increases the ratio of PS-16 PLB to total PLB by 51.23 ± 8.87 % comparing to its basal level (n=10 cells, $P < 0.05$, Fig. 5A). IBMX (example in Fig.

8A) induced a prompt and significant increase in the SAN beating rate. The average increase in the spontaneous beating rate was from 375 ± 18 bpm to 623 ± 7 bpm, (n=6, $P < 0.05$, Fig. 8D). The chronotropic effects of IBMX indicate that an increase in intracellular cAMP level activates PKA and accelerates SAN automaticity, independent of external receptor stimulation. Stated in other terms, these data indicate constitutively activate PDE activity, which degrades cAMP, leads to suppression of downstream cAMP-mediated PKA-dependent signaling. When PDE activity is blunted, PKA dependent signaling and the spontaneous beating rate are markedly enhanced in mouse SAN.

Basal cAMP-PKA signaling drives spontaneous basal SR Ca^{2+} releases in permeabilized ("skinned") mouse SANC

To demonstrate that mouse SANC generate rhythmic spontaneous local Ca^{2+} releases (LCRs) locally, without a change in the membrane potential, we permeabilized intact SANC with 0.01% saponin. Figure 6 demonstrates the presence of spontaneous LCRs on the confocal line scan image in a representative 'skinned' mouse SANC bathed at 100 nM free [Ca^{2+}]. Note, that in control conditions (Figure 6A, top image), spontaneous LCRs are roughly periodic (Figure 6B,) with an average frequency 4.79±1.0 Hz (n=16, not shown). Inhibition of PKA signaling by 15 μM PKI, which decreases PLB phosphorylation, markedly suppresses LCRs (Figure 6A bottom image) and abolishes LCR periodicity (Figure 6B) or rhythmicity, assessed by autocorrelation function (Figure 6C, right top panel). Within 2 minutes, PKI significantly decreases the average LCR number (LCR occurrence within the 100 μm of scan line per 1 second of time), amplitude and size, and the average total Ca^{2+} release of the ensemble of LCRs (LCR signal mass) and rhythmicity index (Figure 6C). When cAMP (1 μM) is added in the continued presence of PKI there is a partial recovery of LCR characteristics including rhythmicity, toward the pre-PKI addition basal level (data not shown).

PDE inhibition by IBMX (5 μM) which leads to an increased PLB phosphorylation (as shown in Figure 4E), increases LCR occurrence (Figure 7A, lower image), and shifts the power spectra (Fig. 7B), and autocorrelation function (Fig. 7C, right top panel) to a higher frequency (Figure 7B). The average effects of PDE on LCR characteristics are shown in Fig. 7C, left panels.

β-AR stimulation of cAMP-PKA signaling increases beating rate and PKA-dependent phosphorylation

As expected, in response to β-AR stimulation (ISO, 1 μM), PLB-PS16 immuno-reactivity increases and the ratio of PLB-PS16 to total PLB increases in mouse SANC (Fig. 4F). Representative example of the ISO effect to increase spontaneous SAN beating rate is shown in Figure S7A. On average, ISO increased the PS16/total PLB immuno-labeling by 68.86 ± 4.54 % from its untreated controls (Fig. 5A, n=14, $p < 0.01$). ISO increased beating rate of SAN by 48.07 ± 3.60 % (Fig. 8D) from 402.72 ± 22.21 bpm to 594.78 ± 28.59 bpm ($n = 6$, $p<0.01$). Also note in Figure 5B, that the relationship of changes in beating rate that accompanies PLB16 phosphorylation in response to β-AR stimulation, PDE inhibition or AC or PKA inhibition forms a linear continuum ($R^2 = 0.85$).

Augmentation of beating rate in response to an increase in cAMP/PKA activation requires intact SR function

Increases in mouse SAN spontaneous beating rate in response to β-AR stimulation or basal PDE inhibition are both linked to an increase in cAMP-mediated PKA-dependent PLB phosphorylation (Figs. 4E,F). The normal increase in beating rate by ISO cannot be maintained at the same level in the presence of impaired SR Ca^{2+} cycling as when SR calcium cycling is intact (Figs. 8D, S7). When intracellular Ca^{2+} cycling is intact, IBMX

(100 μM; Fig. 8A) similar to ISO increases the basal beating rate on average by 63.25 ± 6.62% (n=6, $P < 0.05$, Fig. 8D). When CPA is added in the presence of IBMX the beating rate decreases (representative example in Fig. 8B) on average, from 585 to 396.23 ± 17.08 bpm (i.e. 8.5% decrease comparing to basal level) (n=3, $P < 0.05$, Fig. 8D). Similarly, IBMX added in the presence of CPA fails to have a marked chronotropic effect (Fig. 8C). Thus, the robust acceleration of beating rate in response to β-AR stimulation or PDE inhibition is impaired when SR Ca^{2+} cycling mechanisms are disabled.

DISCUSSION

This is the first study in mouse to comprehensively document: (1) the expression of Ca^{2+} cycling proteins in intact mouse SAN and SANC; (2) a high basal level of PKA-dependent phosphorylation of PLB in mouse SANC; (3) that interfering with or stimulating intrinsic AC-cAMP-PKA-Ca^{2+}-signaling cascade, even in the absence of β-AR mediated stimulation, can, respectively, significantly inhibit or stimulate pacemaking function, indicating a major constitutive role of this signaling cascade in normal automaticity of mouse SAN.

During mouse cardiac cell development, the RyR Ca^{2+} release modulates the spontaneous beating rate of stem cell-derived cardiac myocytes [18]. A previous study of RyR mRNA suggests that relative RyR expression is comparable in mouse SAN and ventricular cells [6]. The present study demonstrates abundant expression of Ca^{2+} cycling proteins in adult mouse SAN that is equivalent to those of contracting myocardium (e.g. atrium and ventricle), and validates functional importance of Ca^{2+} cycling in SAN for basal spontaneous beating.

The present study also demonstrates that SR of mouse SANC with free [Ca^{2+}] clamped in the physiologic range generates spontaneous, rhythmic LCRs via RyRs (Figs. 6, 7) in the absence of surface membrane function. This extends recent observations [19] that describe local diastolic Ca^{2+} releases in mouse SANC, but attribute such release to Ca^{2+}-induced Ca^{2+} release linked to surface membrane potential. Of note, in the later study, no data on the rhythmicity of the observed diastolic Ca^{2+} release are provided. Numerous studies have demonstrated that disabling RyR with ryanodine interferes with normal spontaneous automaticity in SAN or SANC of rabbit [20, 21], dog [22], guinea-pig [23], rat[24], mouse [7, 9, 24] and toad [25]. An inhibitory effect of ryanodine has also been observed in the atrioventricular node (the secondary pacemaker of heart) of mouse [9] and rabbit [26]. Furthermore, normal automaticity of other types of cardiac pacemaker cells, e.g. cat atrial latent pacemaker cells [27], the spontaneous beating rate of stem cell derived cardiac myocytes [18] is also decreased by ryanodine. The negative chronotropic effect of ryanodine is concentration-dependent and time-dependent, and occurs in the presence of intact I_{CaL} or I_f [20, 21]. Thus, Ca^{2+} release via RyRs broadly contributes to pacemaker function of a variety of cells within the heart [28]. An incomplete blockade of pacemaker function by ryanodine or by any other SR Ca^{2+} cycling inhibitor, in the present study and in prior studies [7, 9], can be explained by the robustness of the coupled system of SR Ca^{2+} cycling and surface membrane molecules: when the function of the Ca^{2+} clock is diminished, the Membrane Clock function becomes enhanced (possibly because at long cycle lengths I_f current has more time to activate) [29].

The present study also demonstrates for the first time that (i) the level of PLB phosphorylation is constitutively elevated in mouse SAN cells, as in rabbit or guinea pig SANC [2, 30] and (ii) that this phosphorylation status is modulated by AC-cAMP-PKA signaling [30, 31]. Furthermore, we demonstrate the Ca^{2+} clock operation in skinned mouse cells, as in rabbit SANC, requires PKA-dependent phosphorylation, as the specific PKA inhibitor protein, PKI, markedly suppresses SR-generated LCR's, and this effect is reversed by application of cAMP in the continued presence of PKI (Fig. 6). Our study also

demonstrates that although ventricular myocytes have approximately the same density of NCX, SERCA2 and RyRs as do SANC (Fig. 1B), basal spontaneous Ca^{2+} cycling via these molecules is not driven by a high basal cAMP/PKA signaling (Fig. S6). Our results also demonstrate that constitutively elevated AC-PKA signaling is constrained by constitutively high level of PDE activity, as PDE inhibition increases PKA-dependent phosphorylation of PLB and increases the beating rate. Furthermore, this PKA-dependent response affected by PDE inhibition is suppressed when Ca^{2+} pumping or RyR function, as in other species [3], is disabled. As demonstrated by other studies, most components of the PKA pathway are localized to the narrow region between the sarcolemma and the sub-sarcolemmal regions within the cell. Subcellular targeting of PKA through association with AKAPs facilitates PKA-mediated signaling. This AKAP-directed compartmentalization has been demonstrated in cardiac myocytes [32]. Additionally, the disruption of AKAP-mediated PKA anchoring alters the βAR–stimulated contractile response in cardiac myocytes [33].

The fight-or-flight survival mechanism is affected via the release of the neurotransmitter norepinephrine resulting from cardiac sympathetic nerve signaling. β-AR stimulation of pacemaker cells results in an increase in the spontaneous AP firing rate. Early studies by DiFrancesco *et al.* had been interpreted to indicate that activation of I_f current by elevated intracellular cAMP is the key event linking β-AR stimulation to an increased beating rate [34, 35]. However, the adult HCN4 knockout mice show no impairment in heart rate acceleration during sympathetic stimulation [36, 37]. Most recently a conditional cardiac specific HCN4 knockout in mouse heart caused a marked resting bradycardia. But in response to ISO, or during exercise, although the absolute heart rate or AP firing rate was less in the knockout than in wild type (WT), the absolute change in HR was similar in both KO and WT [38]. The diminished contribution of I_f to AP firing rate regulation in response to sympathetic stimulation could possibly relate to a reduction in channel activation time during short diastolic intervals that accompany an increased beating frequency [29, 39].

More recent studies have embraced the idea that mechanisms other than I_f mediate the chronotropic response to β-AR stimulation [1, 28]. Recent studies demonstrate that other mechanisms may also be involved in β-AR linked acceleration in SANC firing [8, 40]. Wu *et al*., show that CaMKII inhibition selectively reduces the positive chronotropic response in SANC during β-AR stimulation and propose that this signaling cascade is required for fight-or-flight response [8]. Similar to our findings, CaMKII signaling involvement in the increase of the AP firing rate requires intact SR Ca^{2+} cycling. However, unlike the PKA signaling pathway, CaMKII activation was not essential for maintaining basal SAN pacemaker function, as the CaMKII disabled mouse show no change in basal heart rate or SAN beating rate. A most recent study has confirmed the finding that CaMKII also plays a key role for catecholamine-independent increase of the mouse SA node beating rate, but is not required for basal AP firng [40]. SA node cells and entire hearts isolated from transgenic mice with CaMKII inhibited (produced by expression of an inhibitory peptide (AC3-I)) were resistant to BayK, an L-type Ca^{2+} channel agonist, produced acceleration of spontaneous AP firing. Furthermore, Wu *et al.*, also show that ~50% of β-AR stimulation induced increase in HR is CaMKII independent. These studies [8, 40], together with our data, show a multi-pathway regulation of SANC by β-AR stimulation during the fight-or-flight response of mouse pacemaker cells.

Apparent differences between mouse and rabbit SANC in the requirement of basal CaMKII activation for basal AP firing [3, 8, 40] could be based on differences between sets of ionic currents present in these species. In contrast to higher mammals, mice have a high density of Na^+ channels in the sinoatrial node, and suppression of sodium current by TTX produces marked bradycardia in the isolated mouse heart [41]. Heterozygous Scn5a+/- mice showed depressed heart rates and sinoatrial block [5], implicating an important role of Nav1.5

cardiac Na^+ channel in mouse sinoatrial node pacemaking, suggesting a necessity of Nav1.5 to maintain the extremely high heart rate and fast conduction in the mouse heart. In contrast, in rabbit or canine hearts, Na^+ currents do not contribute to normal automaticity of adult isolated SA node cells [42, 43]. Thus, SANC of larger animals, like rabbit, are more dependent on L-type Ca current ($I_{Ca,L}$) to generate an AP upstroke of primary pacemaker cell, and require an amplified $I_{Ca,L}$ to support cardiac pacemaker function, achieved, in part, by basal CAMKII-dependent phosphorylation of L-type Ca channels [41].

It is important to note that, in addition to modulating SR Ca^{2+} cycling, cAMP- and PKA-dependent phosphorylation and Ca^{2+} itself, also regulate the function of surface membrane components, e.g. Ca^{2+} and PKA modulate L-type Ca^{2+} channel and cAMP binds to HCN channels [44]. Thus, the Ca^{2+}-cAMP-PKA signaling in pacemaker cells regulates the function of both membrane and Ca^{2+} clocks. These results in mouse are consistent with other studies in rabbit, dog and frog, supporting an active AC-cAMP-PKA signaling in mouse basal SAN function [1, 28] L-type Ca^{2+} channels, which carry the inward current during SAN action potential, are another downstream target of β-AR stimulation and PKA signaling [45].

Our study, like prior studies in other species [12, 23], shows that inhibition of Ca^{2+} cycling in SAN markedly reduce the basal spontaneous SAN firing rate, and that Ca^{2+} cycling inhibition hampers SAN AP rate acceleration in response to β-AR stimulation, confirming prior studies [7–9]. In other words, β-AR activation of AC-cAMP-PKA-Ca^{2+} utilizes the same signaling mechanisms that execute basal SAN beating via Ca^{2+}. This later result indicates that the β-AR stimulation induced increase in beating rate (fight-or-flight response) requires modulation of intracellular Ca^{2+} cycling [46]. It has been shown that the periodicity of the coupled membrane-Ca^{2+} clock system in rabbit SANC is regulated by the amount of Ca^{2+} available for SR Ca^{2+} pumping (regulated in large part by surface membrane proteins), SERCA function, Ca^{2+} release channel characteristics, and the SR Ca^{2+} content. The cell Ca^{2+} content and thus Ca^{2+} available for SR Ca^{2+} cycling is determined by the surface membrane clock components and by the characteristics of the AP generated by these molecules. Thus, a variety of perturbations of the coupled clock system, either inhibition of SR Ca^{2+} cycling, PKA inhibition, PDE inhibition or β-AR stimulation, evoke changes in the LCR period that predict the spontaneous concomitant AP cycle length [1]. The contribution of PKA-dependent modulation of surface membrane molecules during the β-AR-induced chronotropic response cannot be directly measured during spontaneous SAN or SANC beating. Nevertheless, our data show that in the presence of ryanodine or CPA, β-AR stimulation restores the AP firing rate to its level prior to exposure to these drugs that impair intracellular Ca^{2+} cycling. This clearly indicates that function of a coupled system of Ca^{2+} cycling and surface membrane electrogenic molecules is involved in the β-AR chronotropic response in mouse SAN. The role of the surface membrane ion channels within the system may be actually enhanced at low rates (e.g. in the presence of partial inhibition of Ca^{2+} cycling), in part, because I_f current has more time to activate during longer DD.

Our results show that IBMX, a broad-spectrum PDE inhibitor, significantly increases the SAN beating rate by 63%. The positive chronotropic effect of IBMX was related to cAMP accumulation, due to inhibition of its degradation by PDE. Other studies suggest that PDE subtypes, characterized by differential cAMP affinities and efficacies, may have species-dependent and beta-adrenergic regulation- related roles in pacemaking [3]. Studies on rabbit single SANC show that PDE3, but not PDE4, is constitutively active in the basal state. However, PDE4 becomes activated during cAMP accumulation (e.g. during concomittant PDE3 inhibition [47]). While PDE4 is a dominant PDE subtype in mouse heart [48], the PDE3 inhibitor (0.3 μmol/L cilostomide) increased spontaneous AP firing of the mouse right atrium by 19%, while a PDE4 inhibitor (1 μmol/L rolipram) produced only modest 9%

acceleration of the right atrial AP firing rate [49]. Thus, it is possible, that, similar to the rabbit heart [3], the PDE3 subtype is involved in regulation of the mouse SA node spontaneous AP firing. Given that PDEs play an important role in inhibiting the breakdown of cAMP and in facilitating subsequent phosphorylation of Ca^{2+} cycling regulatory proteins in myocyte, further studies are needed to clarify PDE subtype identities and their functional roles in the chronotropic regulation of pacemaking in mouse SAN.

SUMMARY

Ca^{2+}-AC-PKA signaling directed at both SR Ca^{2+} cycling proteins and surface membrane ion channel proteins (Fig. S1) is crucial both for normal basal spontaneous AP firing in mouse SAN and the chronotropic response to β-AR stimulation.

Supplementary Material

Refer to Web version on PubMed Central for supplementary material.

Acknowledgments

This research was supported entirely by the Intramural Research Program of the NIH, National Institute on Aging. A portion of that support was through a R&D contract with MedStar Research Institute.

Reference List

1. Lakatta EG, Maltsev VA, Vinogradova TM. A Coupled SYSTEM of Intracellular Ca2+ Clocks and Surface Membrane Voltage Clocks Controls the Timekeeping Mechanism of the Heart's Pacemaker. Circ Res. 2010; 106:659–73. [PubMed: 20203315]
2. Vinogradova TM, Lyashkov AE, Zhu W, Ruknudin AM, Sirenko S, Yang D, et al. High Basal Protein Kinase A-Dependent Phosphorylation Drives Rhythmic Internal Ca2+ Store Oscillations and Spontaneous Beating of Cardiac Pacemaker Cells. Circ Res. 2006; 98:505–14. [PubMed: 16424365]
3. Vinogradova TM, Sirenko S, Lyashkov AE, Younes A, Li Y, Zhu W, et al. Constitutive phosphodiesterase activity restricts spontaneous beating rate of cardiac pacemaker cells by suppressing local Ca2+ releases. Circ Res. 2008; 102:761–9. [PubMed: 18276917]
4. Ludwig A, Herrmann S, Hoesl E, Stieber J. Mouse models for studying pacemaker channel function and sinus node arrhythmia. Prog Biophys Mol Biol. 2010; 98:179–85. [PubMed: 19351513]
5. Lei M, Goddard C, Liu J, Leoni AL, Royer A, Fung SSM, et al. Sinus node dysfunction following targeted disruption of the murine cardiac sodium channel gene Scn5a. The Journal of Physiology. 2005; 567:387–400. [PubMed: 15932895]
6. Masumiya H, Yamamoto H, Hemberger M, Tanaka H, Shigenobu K, Chen SRW, et al. The mouse sino-atrial node expresses both the type 2 and type 3 Ca2+ release channels/ryanodine receptors. FEBS Lett. 2003; 553:141–4. [PubMed: 14550562]
7. Ju YK, Chu Y, Chaulet H, Lai D, Gervasio OL, Graham RM, et al. Store-operated Ca2+ influx and expression of TRPC genes in mouse sinoatrial node. Circ Res. 2007; 100:1605–14. [PubMed: 17478725]
8. Wu Y, Gao Z, Chen B, Koval OM, Singh MV, Guan X, et al. Calmodulin kinase II is required for fight or flight sinoatrial node physiology. Proceedings of the National Academy of Sciences. 2009; 106:5972–7.
9. Nikmaram MR, Liu J, Abdelrahman M, Dobrzynski H, Boyett MR, Lei M. Characterization of the effects of Ryanodine, TTX, E-4031 and 4-AP on the sinoatrial and atrioventricular nodes. Prog Biophys Mol Biol. 2007; 96:452–64. [PubMed: 17850852]
10. Younes A, Lyashkov AE, Graham D, Sheydina A, Volkova MV, Mitsak M, et al. Ca2+-stimulated Basal Adenylyl Cyclase Activity Localization in Membrane Lipid Microdomains of Cardiac Sinoatrial Nodal Pacemaker Cells. J Biol Chem. 2008; 283:14461–8. [PubMed: 18356168]

11. Mattick P, Parrington J, Odia E, Simpson A, Collins T, Terrar D. Ca2+-stimulated adenylyl cyclase isoform AC1 is preferentially expressed in guinea-pig sino-atrial node cells and modulates the If pacemaker current. The Journal of Physiology. 2007; 582:1195–203. [PubMed: 17540702]
12. Lyashkov AE, Juhaszova M, Dobrzynski H, Vinogradova TM, Maltsev VA, Juhasz O, et al. Calcium Cycling Protein Density and Functional Importance to Automaticity of Isolated Sinoatrial Nodal Cells Are Independent of Cell Size. Circ Res. 2007; 100:1723–31. [PubMed: 17525366]
13. Liu J, Dobrzynski H, Yanni J, Boyett MR, Lei M. Organisation of the mouse sinoatrial node: structure and expression of HCN channels. Cardiovas Res. 2007; 73:729–38.
14. Vinogradova TM, Zhou YY, Maltsev V, Lyashkov A, Stern M, Lakatta EG. Rhythmic Ryanodine Receptor Ca2+ Releases During Diastolic Depolarization of Sinoatrial Pacemaker Cells Do Not Require Membrane Depolarization. Circ Res. 2004; 94:802–9. [PubMed: 14963011]
15. Song KS, Scherer PE, Tang Z, Okamoto T, Li S, Chafel M, et al. Expression of caveolin-3 in skeletal, cardiac, and smooth muscle cells. Caveolin-3 is a component of the sarcolemma and co-fractionates with dystrophin and dystrophin-associated glycoproteins. J Biol Chem. 1996; 271:15160–5. [PubMed: 8663016]
16. Barbuti A, Terragni B, Brioschi C, DiFrancesco D. Localization of f-channels to caveolae mediates specific [beta]2-adrenergic receptor modulation of rate in sinoatrial myocytes. J Mol Cell Cardiol. 2007; 42:71–8. [PubMed: 17070839]
17. Barbuti A, Gravante B, Riolfo M, Milanesi R, Terragni B, DiFrancesco D. Localization of Pacemaker Channels in Lipid Rafts Regulates Channel Kinetics. Circ Res. 2004; 94:1325–31. [PubMed: 15073040]
18. Yang HT, Tweedie D, Wang S, Guia A, Vinogradova T, Bogdanov K, et al. The ryanodine receptor modulates the spontaneous beating rate of cardiomyocytes during development. Proc Natl Acad Sci U S A. 2002; 99:9225–30. [PubMed: 12089338]
19. Chen B, Wu Y, Mohler PJ, Anderson ME, Song LS. Local control of Ca2+-induced Ca2+ release in mouse sinoatrial node cells. J Mol Cell Cardiol. 2009; 47:706–15. [PubMed: 19615376]
20. Li J, Qu J, Nathan RD. Ionic basis of ryanodine's negative chronotropic effect on pacemaker cells isolated from the sinoatrial node. Am J Physiol. 1997; 273:H2481–H2489. [PubMed: 9374788]
21. Bogdanov KY, Vinogradova TM, Lakatta EG. Sinoatrial nodal cell ryanodine receptor and Na^{+}-Ca^{2+} exchanger: molecular partners in pacemaker regulation. Circ Res. 2001; 88:1254–8. [PubMed: 11420301]
22. Joung B, Tang L, Maruyama M, Han S, Chen Z, Stucky M, et al. Intracellular Calcium Dynamics and Acceleration of Sinus Rhythm by {beta}-Adrenergic Stimulation. Circulation. 2009; 119:788–96. [PubMed: 19188501]
23. Rigg L, Terrar DA. Possible role of calcium release from the sarcoplasmic reticulum in pacemaking in guinea-pig sino-atrial node. Exp Physiol. 1996; 81:877–80. [PubMed: 8889484]
24. Bassani JWM, Godoy CMG, Bassani RA. Effect of ryanodine on sinus node recovery time determined in vitro. Brazilian Journal of Medical and Biological Research. 1999; 32:1039–43. [PubMed: 10454767]
25. Ju YK, Allen DG. Intracellular calcium and Na^{+}-Ca^{2+} exchange current in isolated toad pacemaker cells. J Physiol. 1998; 508:153–66. [PubMed: 9490832]
26. Ridley JM, Cheng H, Harrison OJ, Jones SK, Smith GL, Hancox JC, et al. Spontaneous frequency of rabbit atrioventricular node myocytes depends on SR function. Cell Calcium. 2008; 44:580–91. [PubMed: 18550162]
27. Rubenstein DS, Lipsius SL. Mechanisms of automaticity in subsidiary pacemakers from cat right atrium. Circ Res. 1989; 64:648–57. [PubMed: 2467760]
28. Vinogradova TM, Lakatta EG. Regulation of basal and reserve cardiac pacemaker function by interactions of cAMP-mediated PKA-dependent Ca2+ cycling with surface membrane channels. J Mol Cell Cardiol. 2009; 47:456–74. [PubMed: 19573534]
29. Liu J, Noble PJ, Xiao G, Abdelrahman M, Dobrzynski H, Boyett MR, et al. Role of pacemaking current in cardiac nodes: Insights from a comparative study of sinoatrial node and atrioventricular node. Prog Biophys Mol Biol. 2007; 96:294–304. [PubMed: 17905415]

30. Mattick P, Parrington J, Odia E, Simpson A, Collins T, Terrar D. Ca2+-stimulated adenylyl cyclase isoform AC1 is preferentially expressed in guinea-pig sino-atrial node cells and modulates the If pacemaker current. The Journal of Physiology. 2007; 582:1195–203. [PubMed: 17540702]
31. Younes A, Lyashkov AE, Graham D, Sheydina A, Volkova MV, Mitsak M, et al. Ca2+-stimulated Basal Adenylyl Cyclase Activity Localization in Membrane Lipid Microdomains of Cardiac Sinoatrial Nodal Pacemaker Cells. J Biol Chem. 2008; 283:14461–8. [PubMed: 18356168]
32. Marx SO, Reiken S, Hisamatsu Y, Jayaraman T, Burkhoff D, Rosemblit N, et al. PKA phosphorylation dissociates FKBP12. 6 from the calcium release channel (ryanodine receptor): defective regulation in failing hearts. Cell. 2000; 101:365–76. [PubMed: 10830164]
33. Fink MA, Zakhary DR, Mackey JA, Desnoyer RW, Apperson-Hansen C, Damron DS, et al. AKAP-Mediated Targeting of Protein Kinase A Regulates Contractility in Cardiac Myocytes. Circ Res. 2001; 88:291–7. [PubMed: 11179196]
34. Brown HF, DiFrancesco D, Noble SJ. How does adrenaline accelerate the heart? Nature (London). 1979; 280:235–6. [PubMed: 450140]
35. DiFrancesco D. The contribution of the 'pacemaker' current (if) to generation of spontaneous activity in rabbit sino-atrial node myocytes. The Journal of Physiology. 1991; 434:23–40. [PubMed: 2023118]
36. Herrmann S, Stieber J, Stockl G, Hofmann F, Ludwig A. HCN4 provides a /'depolarization reserve/' and is not required for heart rate acceleration in mice. EMBO J. 2007; 26:4423–32. [PubMed: 17914461]
37. Hoesl E, Stieber J, Herrmann S, Feil S, Tybl E, Hofmann F, et al. Tamoxifen-inducible gene deletion in the cardiac conduction system. J Mol Cell Cardiol. 2008; 45:62–9. [PubMed: 18538341]
38. Baruscotti M, Bucchi A, Viscomi C, Mandelli G, Consalez G, Gnecchi-Rusconi T, et al. Deep bradycardia and heart block caused by inducible cardiac-specific knockout of the pacemaker channel gene Hcn4. Proceedings of the National Academy of Sciences. 2011; 108:1705–10.
39. Maltsev VA, Lakatta EG. Synergism of coupled subsarcolemmal Ca2+ clocks and sarcolemmal voltage clocks confers robust and flexible pacemaker function in a novel pacemaker cell model. AJP - Heart and Circulatory Physiology. 2009; 296:H594–H615. [PubMed: 19136600]
40. Gao Z, Singh MV, Hall DD, Koval OM, Luczak ED, Joiner Ml, et al. Catecholamine-Independent Heart Rate Increases Require CaMKII. Circulation: Arrhythmia and Electrophysiology. 2011
41. Maier SKG, Westenbroek RE, Yamanushi TT, Dobrzynski H, Boyett MR, Catterall WA, et al. An unexpected requirement for brain-type sodium channels for control of heart rate in the mouse sinoatrial node. Proc Natl Acad Sci U S A. 2003; 100:3507–12. [PubMed: 12631690]
42. Baruscotti M, DiFrancesco D, Robinson RB. A TTX-sensitive inward sodium current contributes to spontaneous activity in newborn rabbit sino-atrial node cells. The Journal of Physiology. 1996; 492:21–30. [PubMed: 8730579]
43. Protas L, Oren RV, Clancy CE, Robinson RB. Age-dependent changes in Na current magnitude and TTX-sensitivity in the canine sinoatrial node. J Mol Cell Cardiol. 2010; 48:172–80. [PubMed: 19665465]
44. Mangoni ME, Nargeot J. Genesis and Regulation of the Heart Automaticity. Physiol Rev. 2008; 88:919–82. [PubMed: 18626064]
45. Qu Y, Baroudi G, Yue Y, El-Sherif N, Boutjdir M. Localization and modulation of alpha1D (Cav1. 3) L-type Ca channel by protein kinase A. American Journal of Physiology - Heart and Circulatory Physiology. 2005; 288:H2123–H2130. [PubMed: 15615842]
46. Vinogradova TM, Bogdanov KY, Lakatta EG. β-Adrenergic stimulation modulates ryanodine receptor Ca^{2+} release during diastolic depolarization to accelerate pacemaker activity in rabbit sinoatrial nodal cells. Circ Res. 2002; 90:73–9. [PubMed: 11786521]
47. Vinogradova TM, Lyashkov AE, Spurgeon H, Lakatta EG. Local Ca Releases And Spontaneous Beating Rate Of Rabbit Sinoatrial Node Cells Are Controlled By Interaction Of Basal Phosphodiesterase 3 And 4 Activity. Circulation. 2008; 118:S343.
48. Osadchii O. Myocardial Phosphodiesterases and Regulation of Cardiac Contractility in Health and Cardiac Disease. Cardiovascular Drugs and Therapy. 2007; 21:171–94. [PubMed: 17373584]

49. Galindo-Tovar A, Kaumann AJ. Phosphodiesterase-4 blunts inotropism and arrhythmias but not sinoatrial tachycardia of (beta)-adrenaline mediated through mouse cardiac beta-1-adrenoceptors. Brit J Pharmacol. 2008; 153:710–20. [PubMed: 18084319]

Highlights

- PKA signaling drives basal pacemaker function in mouse sinoatrial node
- PKA-dependent rhythmic spontaneous Ca^{2+} cycling drives mouse heart pacemakers
- Ca^{2+} oscillations generate normal automaticity in mouse sinoatrial node cells

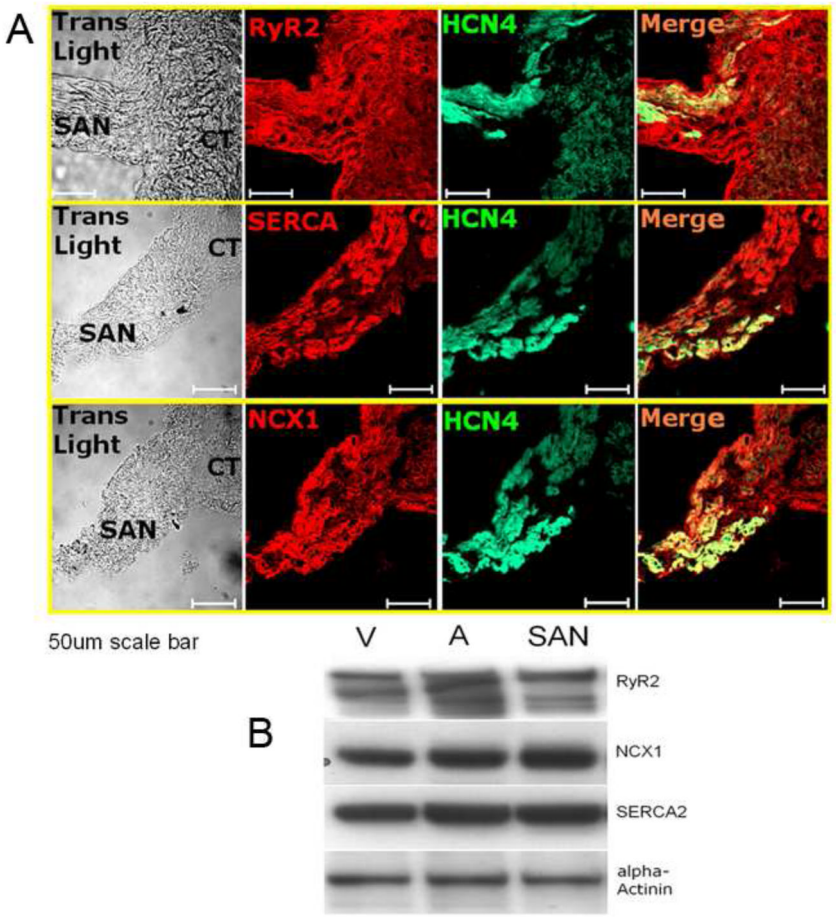

Figure 1.

Molecular phenotype of Ca^{2+} cycling proteins in mouse SAN/SANC. A. Abundant expressions of RyR2, SERCA2 and NCX1 protein are found in both SAN region and neighboring atrium (scale=50 μm); B. Western blots of SAN, atrial and ventricular tissue for RyR2, SERCA2a and NCX1 confirm abundant quantities are expressed in SAN compared to contracting myocardium. Note that SAN strips pooled from mice are required for western blots.

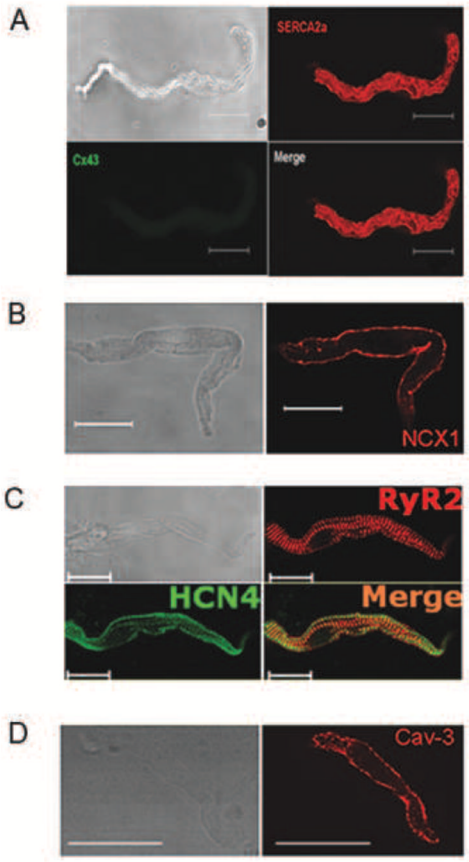

Figure 2.
Isolated mouse SANC with positive immuno-labeling of SERCA2 (A), NCX1 (B), RyR2 and HCN4 (C), Cav-3 (D) with their specific patterns. Note SANC are negative for Cx43 (A) and HCN4 (green) and RyR2 (red) co-localize in SANC (C) sub-sarcolemmal area (scale=20 μm).

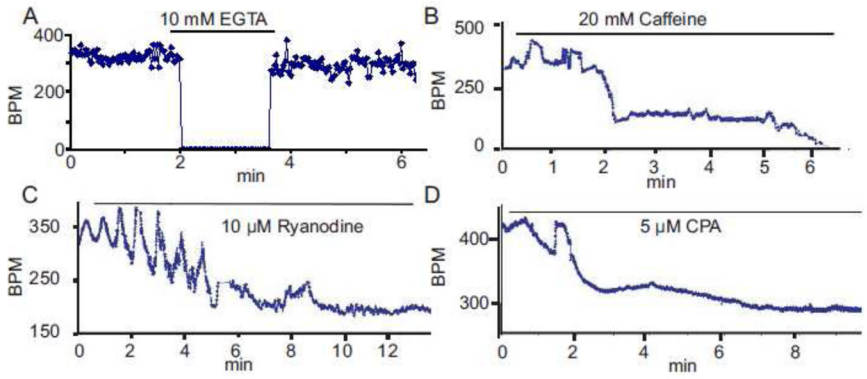

Figure 3.

SAN pacemaking function depends on intact SR Ca^{2+} function. Change of spontaneous beating SAN rate under: removal of calcium by Ca^{2+}-free Tyrode solution (A); depleting SR Ca^{2+} content by 20 mM caffeine (B); inhibition of Ca^{2+} releasing from SR by ryanodine (C); inhibition of Ca^{2+} pumping into SR by CPA (D).

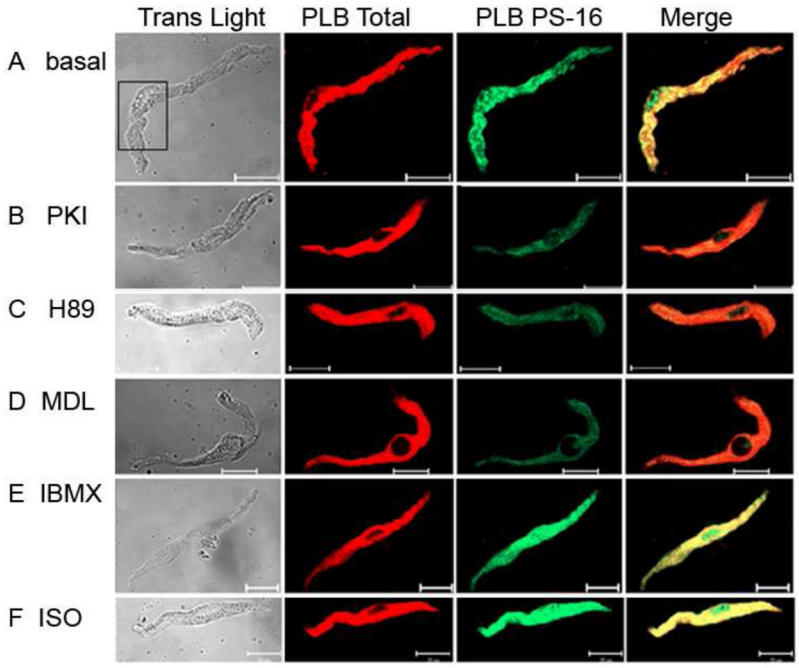

Figure 4.

AC-cAMP-PKA dependent PLB phosphorylation in mouse SANC. A: Immuno-reactivity change of PLB-PS16 (green) and PLN total (red) in untreated SANC (basal, A), PKA inhibition (PKI, B and H89, C), AC inhibition (MDL, D), PDE inhibition (IBMX, E) and β-AR stimulation (ISO, F), scale = 20 μm.

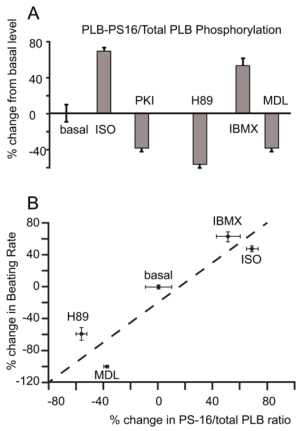

Figure 5.

A. The average change in PS-16/total PLB ratio is shown in the bar graph. B. The relationship of changes in beating rate to changes in PLB16 phosphorylation in response to β-AR stimulation, PDE inhibition or PKA inhibition comparing to the basal level.

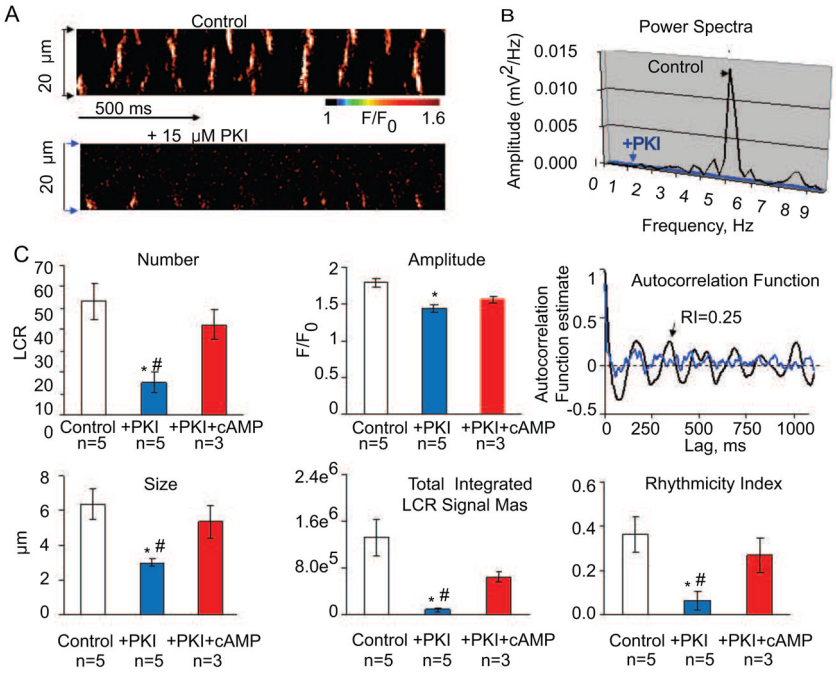

Figure 6.

Basal cAMP-PKA signaling drives rhythmic spontaneous basal local SR Ca^{2+} releases in permeabilized mouse SANC. A. Confocal linescan images of a representative skinned mouse SANC bathed in 100 nM free Ca^{2+} before (top) and during superfusion with 15 μM PKI (bottom). B. Power spectrum of a continuous 4 second recording of LCRs (the average signal in A between two arrows) in panel A. C. Autocorrelation function (right panels) and comparison of average LCR characteristics in control conditions and during application of 15 μM PKI and 1 μM of cAMP in the presence of 15 μM PKI: number (normalized per 1 second and 100 μm); amplitude (F/F0); size (FWHM), measured as full width at half maximum amplitude; total integrated LCR signal mass (product of the LCR size, amplitude, duration, (see online supplement for details), rhythmicity index (RI) (estimated from the amplitude of the third peak of the autocorrelation function). Bars are mean±SEM, *P<0.05 PKI vs. control.

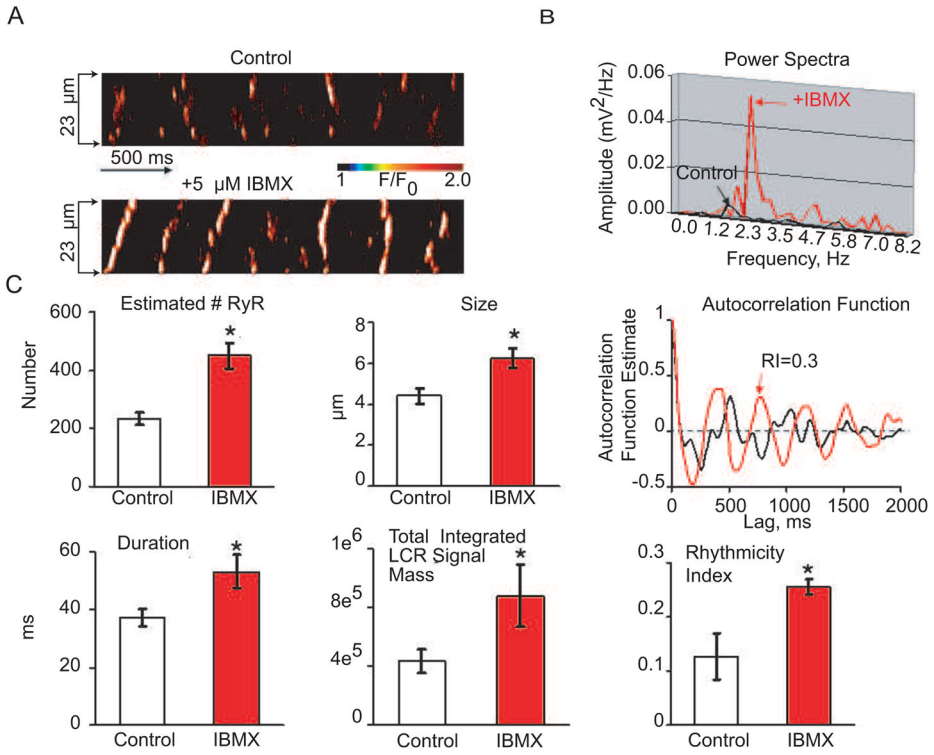

Figure 7.

PDE inhibition accelerates rhythmic spontaneous basal local SR Ca^{2+} releases in permeabilized mouse SANC. A, Confocal linescan images of a representative skinned mouse SANC bathed in 100 nM free Ca^{2+} before (top) and during exposure to 5 μM IBMX (bottom). B, Power spectrum of a continuous 4-s-long recording of LCRs (for the average signal between two arrows in panel A. C, Autocorrelation function and comparison of average LCR characteristics in control conditions and after 5 μM IBMX: A crude index to estimate normalized number of activated RyR within an LCR (see the supplementary method); size (FWHM), measured as full width at half maximum amplitude; duration (FDHM) measured as the full duration at half-maximum amplitude; total integrated LCR signal mass (normalized sum of size, amplitude, duration, see the method part), rhythmicity index (RI) (estimated from the amplitude of the third peak of the autocorrelation function). Bars are mean±SEM, *P<0.05.

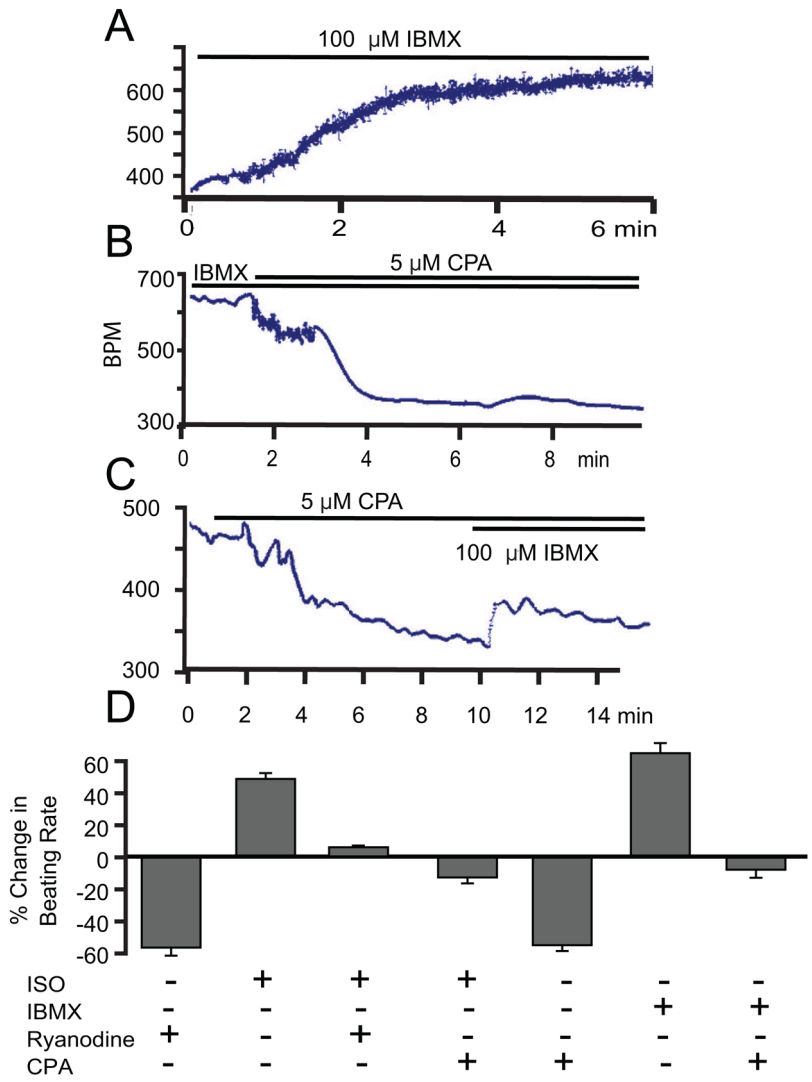

Figure 8.

Augmentation of beating rate in response to an increase in cAMP/PKA activation requires intact SR function. Beating rate increase in response to IBMX (A) and is significantly blunted in the presence of inhibition of SR Ca^{2+} pumping by CPA (B and C). The average responses in beating rate to IBMX or ISO in the presence or absence of CPA or ryanodine (D).